Earthquake Engineering, Tenth World Conference © 1992 Balkema, Rotterdam. ISBN 90 5410 060 5

Incremental constitutive law for sand: Anisotropic and cyclic effects

H. Di Benedetto, O. Hameury & G. B. Cazacliu
Laboratoire Géomatériaux, Ecole Nationale des Travaux Publics de l'Etat, Vaulx en Velin, France

ABSTRACT: First we present a constitutive law of the "interpolation type". Then the hollow cylinder for sand developed at the "Géomatériaux" laboratory of the Ecole Nationale des Travaux Publics de l'Etat is described. At least comparisons between cyclic shear tests with and without rotation of principal axes, and simulations using the incremental law are proposed.

1 INTRODUCTION

During an earthquake the different created waves (body, surface) induce in the ground a field of strain and stress rapidly changing with time. Various in situ measurements show that the cyclic strain may reach more than 10-3 m/m. There is a great number of cycles.

Generally, the solicitation includes the rotations of principal axes.

Considering these physical observations, for correctly modeling the movement of the ground during an earthquake, it is necessary to describe the behavior of soil considering : rotation of solicitation, cyclic effects, anisotropy, stress path history.

We propose in this article a study on the experimental observations and description of the behavior of sand. We focus on the phenomena underlined before. It is divided into three parts :

First the general formalism of the incremental law proposed by Di Benedetto (1987), which does not suppose any elastic or plastic decomposition, is presented. New developments about description of the anisotropy, cyclic effects and stress path history, following observations of recent experimental works on sand within the French "Greco Géomatériaux (soils, concretes, rocks)" are introduced.

Then the hollow cylinder apparatus developed at the "Géomatériaux" laboratory of the "Ecole Nationale des Travaux Publics de l'Etat" is described.

At least comparisons between cyclic shear tests and simulations using the incremental law are proposed.

2 DESCRIPTION OF THE LAW

General theory shows that, for "Simple Thermo-mechanical Materials", the Kirchhoff stress tensor ($\underline{T}$) at a material point (X) can be expressed as a functional of the strain tensor ($\underline{\varepsilon}$), the temperature (θ) and the temperature gradient (gradθ) histories, Eringen (1975):

$$\underline{T}(X, t) = \hat{\underline{T}}_{\chi}(\underline{\varepsilon}(t'), \theta(t'), \mathrm{grad}\theta(t') ; X); \; t' \leq t \quad (1)$$

The development of numerical codes (F.E.M.,...) leads to the utilization of an incremental formulation for the constitutive law. A general incremental formulation is obtained with the application of the determinism principle during a time increment (δt) and allows the introduction of a function (f_1), Di Benedetto (1987) :

$$f_1(\underline{\delta\varepsilon}, \delta\theta, \delta\mathrm{grad}_t\theta, \delta t) - \underline{\delta\sigma} = \underline{0} \quad (2)$$

Where

f_1 is a symmetrical tensorial function of order 2

$\underline{\delta\sigma}$ is a stress increment ($= \underline{\dot{\sigma}}\ \delta t$)

$\underline{\delta\varepsilon}$ is a strain increment ($= \underline{D}\ \delta t$)

$\delta\mathrm{grad}_t\theta$ is a temperature gradient increment

($= \mathrm{gr\dot{a}d}_t\theta\ \delta t$)

$\delta\theta$ is a temperature increment ($= \dot{\theta}\ \delta t$)

$\underline{D}$ is the stain rate tensor

"·" denote an objective derivative, such as the intrinsic or the Jaumann's derivatives.

f_1 depends on the "state" of the material. This state is characterized with the history parameters (h).These parameters allow to take into account the stress path induced anisotropy.

We consider a linearized form of equation (2) Di Benedetto (1987) :

$$\underline{\delta\varepsilon} = \underline{\delta\varepsilon}^{nv} + \underline{\delta\varepsilon}^{v} + \underline{\delta\varepsilon}^{\theta} + \underline{\delta\varepsilon}^{\mathrm{grad}\theta} \quad (3)$$

Where $\underline{\delta\varepsilon}^{nv}$ is the instantaneous or non viscous strain increment

$\underline{\delta\varepsilon}^{v}$ is the deferred or viscous strain increment

$\underline{\delta\varepsilon}^{\theta}$ is the strain increment produced by a variation of temperature

$\underline{\delta\varepsilon}^{\mathrm{grad}\theta}$ is the strain increment produced by a variation of the temperature gradient.

This linearized form means that non viscous, viscous and temperature effects are incrementally independent. But these effects may be coupled because each of them produces a variation of the history parameters (h).

The temperature is introduced as a solicitation parameter in the term $\underline{\delta\varepsilon}^{\theta}$ but the temperature is an history parameter for the description of the term $\underline{\delta\varepsilon}^{v}$. It is well known that experimentally the viscous properties of material change when considering constant but different temperatures.

In this article, as we consider sand, only the first term of equations (3) is presented.

Description of the non viscous part

It can be shown for non viscous geomaterials, Darve (1978), that the general form of the non viscous deformation increment is :

$$\underline{\delta\varepsilon}^{nv} = \underline{M}(\underline{\delta\hat{\sigma}}, h)\,\underline{\delta\sigma} \qquad (4)$$

where $\underline{\delta\hat{\sigma}}$ symbolizes the "direction" of $\underline{\delta\sigma}$:

$$\underline{\delta\hat{\sigma}} = \underline{\delta\sigma} / \| \underline{\delta\sigma} \| = \underline{\dot{\sigma}} / \| \underline{\dot{\sigma}} \|$$

$\| \underline{\delta\sigma} \|$ is the norm of $\underline{\delta\sigma}$ $((\Sigma\, \delta\sigma_{ij}^{2})^{.5})$

and $\underline{M}$ is the "non viscous" tensor. h represents the whole history parameters also called memory, hardening, state, ... parameters.

The introduction of $\underline{\delta\hat{\sigma}}$ express the irreversibility and the parameters h which may be scalars, vectors or tensors describe the stress history dependence.

A classification of the non viscous laws is possible with respect with the number of discrete values taken by $\underline{M}$ when $\underline{\delta\hat{\sigma}}$ describes the whole increment stress space. For example $\underline{M}$ has only one value for elastic laws, 2 different values for elastoplastic laws with one yield surface, 4 different values for elastoplastic laws with 2 yield surfaces,...

We propose a non viscous part of the law among the "Interpolation type law" frame.

For this type of law, quite different from classical elastoplastic type, the two main aspects are :

1) The obtaining, after a given stress path history, of 6 particular strain increments $\underline{\delta\varepsilon}^{nv}$ ($\underline{\delta\varepsilon}^{1+}$, $\underline{\delta\varepsilon}^{2+}$, $\underline{\delta\varepsilon}^{3+}$, $\underline{\delta\varepsilon}^{1-}$, $\underline{\delta\varepsilon}^{2-}$, $\underline{\delta\varepsilon}^{3-}$) corresponding respectively to 6 particular stress increments ($\underline{\delta\sigma}^{1+}$, $\underline{\delta\sigma}^{2+}$, $\underline{\delta\sigma}^{3+}$, $\underline{\delta\sigma}^{1-}$, $\underline{\delta\sigma}^{2-}$, $\underline{\delta\sigma}^{3-}$). This aspect concerns the description of the "state" of the material (with parameters h). It introduces the history dependence including anisotropy. The 6 particular $\underline{\delta\varepsilon}^{nv}$ are given by 2 (3x3) matrix $\underline{N}^{+}$ and $\underline{N}^{-}$ only function of the history parameters (h). Consequently the stress path history is introduced by the 2 matrix N^{+} and N^{-}.

2) The obtaining using an interpolation rule of the non viscous strain increment response ($\underline{\delta\varepsilon}$) to a given stress increment ($\underline{\delta\sigma}$)(generally different of the 6 particular stress increments considered above) figure 1. This second aspect introduces the irreversibility of the material. Formally this irreversibility is given because of the dependence of $\underline{M}$ with the direction of $\underline{\delta\sigma}$ ($\underline{\delta\hat{\sigma}}$).

Different interpolation rules are proposed, Darve (1978), Chambon (1981), Di Benedetto (1981) and (1987), Royis (1986), Doanh et al (1987), ...A discussion about the apparition of a lack of the one-to-one properties of the law linked with the choice of the interpolation rule is proposed by Royis 1986.

In a general way when strain softening appears the laws may lose their biunivocity. Two different strain increments may give the same stress increment.

Considering these two aspects one can observe the great possible evolution of the law. The simplest form is to consider $\underline{N}^{+} = \underline{N}^{-}$ equal to the isotropic elastic Hooke tensor, then the law is isotropic elastic.

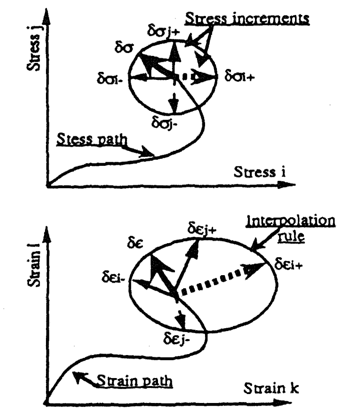

Fig.1 Visualization of the interpolation rule

The description of the proposed law lies on 4 hypotheses which respect the general principles and express the physical observations.

In the following, we will replace second order symmetrical tensors of the space ($\mathbb{E}3$) by vectors of a six dimensional space ($\mathbb{E}6$). In our notation, tensors are underlined while vectors or scalars are not.

H1 : We consider that the "non viscous" tensor $\underline{M}$ has the form precised in the equation (5) when expressed in a set of objective axes ($\vec{p}_i$). We chose the principal axes of the Almansi strain tensor. In the following we reason in these axes.

$$\underline{M} = \left| \begin{array}{cccccc} A & F & E & & & \\ F' & B & D & & 0 & \\ E' & D' & C & & & \\ & & & 2\,G1 & & \\ & 0 & & & 2\,G2 & \\ & & & & & 2\,G3 \end{array} \right| \qquad (5)$$

H2 : The values M_{ij} ($i \le 3$, $j \le 3$) are obtained with an interpolation function for a given "direction" of the stress increment ($\delta\hat{\sigma}$).

The interpolation is done between the 6 strain increments ($\delta\varepsilon^{1+}$, $\delta\varepsilon^{2+}$, $\delta\varepsilon^{3+}$, $\delta\varepsilon^{1-}$, $\delta\varepsilon^{2-}$, $\delta\varepsilon^{3-}$) given respectively by the 6 stress increments ($\delta\sigma^{1+}$, $\delta\sigma^{2+}$, $\delta\sigma^{3+}$, $\delta\sigma^{1-}$, $\delta\sigma^{2-}$, $\delta\sigma^{3-}$) corresponding to "loading" or "unloading" in each direction ($\vec{p}_i$) :

• for "loading" in the direction $\vec{p}_I$; the components of $\delta\sigma^{I+}$ are : $\delta\sigma_i^{I+} = \|\delta\sigma\| \ \delta_{Ii}$ $\quad I \leq 3 ; i \leq 6$

The stress increment is then a simple compression in the direction $\vec{p}_I$. (for example $\delta\sigma^{2+}= (0,\|\delta\sigma\|,0,0,0,0)$)

• for "unloading" in the direction $\vec{p}_I$; the components of $\delta\sigma^{I-}$ are : $\delta\sigma_i^{I-} = -\|\delta\sigma\| \ \delta_{Ii}$ $\quad I \leq 3 ; i \leq 6$

The stress increment is then a simple extension in the direction $\vec{p}_I$. (for example $\delta\sigma^{3-}= (0,0,-\|\delta\sigma\|,0,0,0)$)

where I is fixed and (δ_{Ii}) is the Kronecker symbol; $\delta_{ii} = 1$ and $\delta_{ij} = 0$ if $i \neq j$.

The strain increment is then : $\delta\varepsilon^{I\zeta}= \underline{N}^{\zeta} \ \delta\sigma^{I\zeta}$ (6)

or replacing $\delta\sigma^{I\zeta}$ by its value: $\delta\varepsilon_i^{I\zeta}= \zeta\|\delta\sigma\| \ N_{iI}^{\zeta}$

where ζ is the sign "+" or the sign "-" and I, i, $j \leq 3$

Obviously, $M_{iI} = N_{iI}^{\zeta}$ when the stress increment is : $\delta\sigma^{I\zeta}$.

The obtainment of the eighteen values N_{iI}^{ζ}, giving the strain increment for the 6 special solicitation stress increments is precised in the third hypothesis.

For the calculus on sand we mainly focus on the description of the induced anisotropy (introduced in functions f, g, h, see hypothesis 3) and use the simplest existing interpolation rule proposed by Darve (1978). This rule leads to the existence of 8 different values for the non viscous tensor $\underline{M}$:

$M_{ij}=(N_{ij}^{+} - N_{ij}^{-})/2 * \mathrm{sgn}(\delta\sigma_j) + (N_{ij}^{+}+ N_{ij}^{-})/2$ (7)

<u>H3</u> : The third hypothesis gives the determination of the 18 values N_{ij}^{ζ} (ie : N_{ij}^{+}, N_{ij}^{-}). These values are obtained with the derivation of 3 functions f, g, h specifying the evolution into the axes ($\vec{p}_i$) of principal stress and strain for a stress path, where only one stress is not constant :

$$\Delta\sigma_I = f(\Delta\varepsilon_I)$$
$$\Delta\varepsilon_J = g(\Delta\varepsilon_I) \qquad (8)$$
$$\Delta\varepsilon_K = h(\Delta\varepsilon_I)$$

where I, J, K are different and lower than 4 . The stress components other than σ_I are kept constant.

$\Delta\sigma_I = \sigma_I - \sigma_{invI}$; σ_{invI} is an inversion stress, obtained by a special algorithm, introduced in the direction I to describe cyclic behavior. $\Delta\varepsilon_I$, $\Delta\varepsilon_J$, $\Delta\varepsilon_K$, are obtained from $\Delta\sigma_I$ and respectively f, g, h.

Derivation of (8) gives :

$$\delta\sigma_I = f' \ \delta\varepsilon_I ; \delta\varepsilon_J = g' \ \delta\varepsilon_I ; \delta\varepsilon_K = h' \ \delta\varepsilon_I \qquad (9)$$

The identification of equation (9) with equation (6), for the 3 values (I= 1, 2, 3), gives immediately the 18 values N_{JI}^{ζ} : $N_{II}^{\zeta} = 1/f'$, $N_{KI}^{\zeta} = g'/f'$, $N_{JI}^{\zeta} = h'/f'$, with ζ=sign ($\Delta\sigma_I$) and I,J,K, fixed but different.

The 3 functions f, g, h have general analytical expressions obtained from analysis of triaxial experiments. Between 10 and 19 constants following the desired sophistication (ie description of monotonic or cyclic behavior, anisotropy,...) are needed to express these 3 functions, Di Benedetto (1987), Doanh and al (1987). For the simulations proposed in the fourth paragraph a new formulation from Di Benedetto (1991), where 19 constants have to be given, is presented.

<u>H4</u> : This hypothesis allows to take into account the strain and stress principal axes rotations by the specification of the 3 values M_{ii} for 3<i<7.

Considerations about material invariance for special symmetric cases lead us to propose by extension, for example for M_{44} :

$$M_{44} = [M_{22} + M_{33} - (M_{32}+M_{23})] / 4 \qquad (10)$$

M_{55} and M_{44} are given from (10) by permutation.

We think that the specification of these 3 M_{ii} had to be treated in the same time as hypothesis 3, with the introduction of a general 6 dimensional interpolation function. But, at the present time, the lack of experimental results for solicitation with rotation of principal axes does not allow this.

In fact, we are aware that our fourth hypothesis is quite perfectible because of this lack. This explain why we developed, at "Géomatériaux" laboratory torsion experiments on hollow cylinders for sand and clay. The apparatus for sand is rapidly described in the next paragraph. A new hollow cylinder apparatus, able to apply "little" strain cycles ($10^{-5} < \|\varepsilon\| < 10^{-3}$) from any point of the stess-strain curve, is actually in construction. This apparatus will allow to study "pseudo-elastic" properties of sand.

2 HOLLOW CYLINDER APPARATUS OF ENTPE

A hollow cylinder apparatus working on sand has been developed in the "Géomatériaux" laboratory of ENTPE since 1983. Studies on the influence of the rotation of the principal stress axes and on the anisotropic behavior were performed (Kharchafi 1988, Hameury et al 1991, ...).

This apparatus shown on figure 2, has the following principal characteristics:

- Two samples with different sizes can be prepared. These samples have the same section and different heights; outer diameter: 18 cm, inner diameter: 15 cm, heights of 9 or 18 cm.
- During the tests, 8 measures are performed: the axial displacement, the inner and outer diameter variation, the distortion, the axial strength, the torsion torque, the volume change and/or the pore pressure (figures 2, 3 & 5).
- All these measurements, except the outer diameter variation, are automatically registered by electronic data acquisition system. This system can enable in the same time the automatic conduction of the tests.

All the tests presented bellow, were achieved with

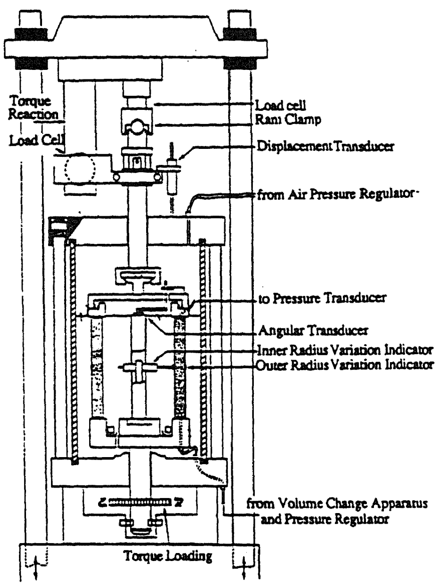

Fig.2 ENTPE hollow cylinder apparatus (schematized)

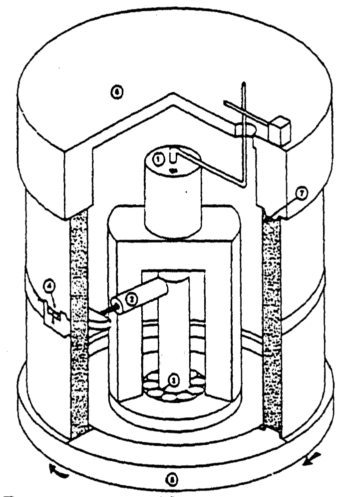

1 Angular Transducer
2 Inner Radius Variation Indicator
3 Ball bearing
4 Outer Radius Variation Indicator
5 Lower base plate
6 Upper base plate
7 Sample

Fig.3 Hollow cylinder sample with the measurement systems

completely saturated Hostun fine sands (RF). This sand is used by the different teams of the French "Gréco Géomatériaux". The inner and outer pressures were always equal: $p_o = p_i = \sigma_r = \sigma_\theta$ (figure 5).

3 COMPARISON BETWEEN THEORY AND EXPERIMENTAL RESULTS

Examples of comparisons between numerical results deduced from the law and homogeneous experiments are proposed below.

We focus on the description of the cyclic effects and of the anisotropy due to the stress path history. A comparison between two types of stress paths with undrained conditions are presented:

a) triaxial undrained tests after different stress path histories. For this kind of test description of the induced anisotropy is the most important.

b) cyclic tests with rotation of principal axes (hollow cylinder samples). For these tests, performed in our laboratory, the cyclic effects and the rotation of principal axes had to be correctly modeled.

Let us underline that one of the interest of the law is the adaptability to various kind of materials and the choice of the degree of complexity we want to simulate.

A new formulation of the f, g, h functions (equation 8) proposed by Di Benedetto (Di Benedetto et al 1991) is introduced to describe anisotropy and cyclic behavior. The stress path history is taken into account by the following history parameters : actual stress (σ), principal axes of the strain tensor (hypothesis 1), new or new define inversion stress (σ_{inv}) and inversion strain (ε_{inv}), and deviatoric strain part. Let us notice that the formulation respects the experimentally observed property (Lanier 1988-90, Kharchafi 1988, ...), that sand "forgets" previous anisotropy when a large deformation is applied.

The number of constants of the law is 19. If we consider that the density has a short variation and choose the parameters only function of the initial density only 14 constants are needed. 16 of these constants can be obtained with 3 classical compression triaxial tests with large unloading (2 different cell pressures and 2 different void ratios) and 1 classical extension triaxial tests with large compression. While the 3 constants of the deviatoric rules need real triaxial stress paths (Cazacliu 1991). In fact, we propose 3 constants values for the sands obtained from Goldsheider (1982) and Lanier (1988, 1989) experimental results.

Triaxial undrained tests

We simulate the behavior of dense Hostun RF sand, following the stress paths performed by Lanier et al (1992), fig 4. The objective of these tests was to show the influence of a previous drained cycle, which creates an induced anisotropy, on the behavior during an undrained compression or extension test; three types of initial state are considered:

1) isotropic drained consolidation until the test value P=0,5 MPa

2) path n°1 then triaxial drained cyclic loading along the direction Y (maximum strain 6%)

3) path n°1 then triaxial drained cyclic loading along the direction Z (maximum strain 6%)

The experimental curves of figure 4, from Lanier et al 1992, represent, in the mean effective stress (P) - deviatoric stress (q) axes, 3 undrained compressions (q>0) and 3 undrained extensions (q<0) along the direction Z obtained respectively after the stress path n° 1, 2 and 3.

One can see the differences due to the previous induced anistropy. For example:

- the sample n°2 in compression has less shear strength than the others and reach the "limit" line at a lower deviatotic stress.

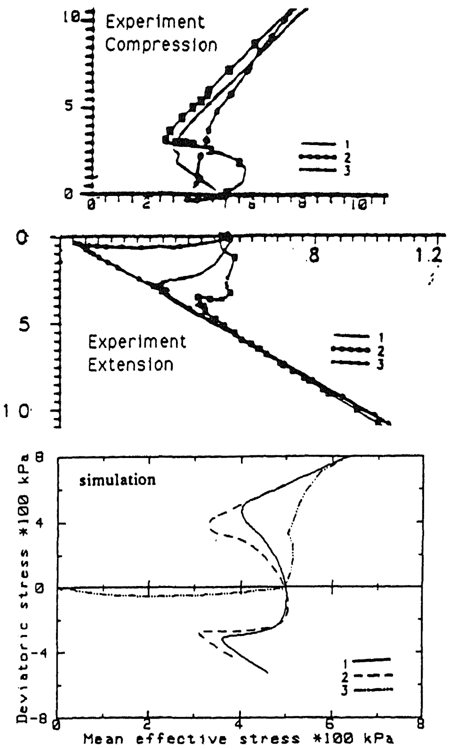

Fig. 4 triaxial undrained tests ($\sigma 2$=0.5 MPa) after different induced anisotropy.

- the sample n°3 in extension liquefy while the others do not.

The accuracy between the experimental data and the simulations with our law is quite satisfactory (figure 4). The modification of the evolution of the effective stresses due to the induced anisotropy seems being obtained.

Cyclic tests with rotation of principal axes

The tests with rotation of principal axes have been achieved on the apparatus presented in the third paragraph. The following loading paths are applied : first triaxial compression, and then cyclic torsional loadings, both under undrained conditions. This stress path involves cyclic rotations of stress and strain principal axes (respectively $\alpha\sigma$ and $\alpha\varepsilon$), due to the initial axial stress (σ_a) which is maintained constant (figure 5):

$$tg\ 2\alpha_\sigma = 2\tau_{a\theta} / (\sigma_a - \sigma_\theta)$$

$$tg\ 2\alpha_\varepsilon = \gamma / (\varepsilon_a - \varepsilon_\theta).$$

For the tests presented below, the sample is prepared dry by pluviation, and tamped by layers to obtain high densities. Then specimen is saturated by carbon dioxide and deaired water to achievc a complete saturation. The obtained Skempton parameter is greater than 0.95. The mean void ratio is 0.65.

Tests begin at the same consolidation stress: 200 kPa. The dimensions of the sample are: height 18 cm, inner diameter 15 cm, outer diameter 18 cm.

The stress path is schematized in figure 5. The cell pressure is kept constant at 200 kPa.

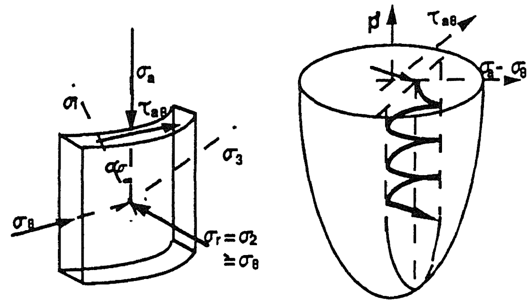

Fig. 5 Applied stress (right) and stress path (left)

Figures 6 to 8 show comparisons between cyclic experimental results and calculus with the law, in the axes: axial minus radial stresses (σ_a-σ_θ) - shear stress ($\tau_{a\theta}$).

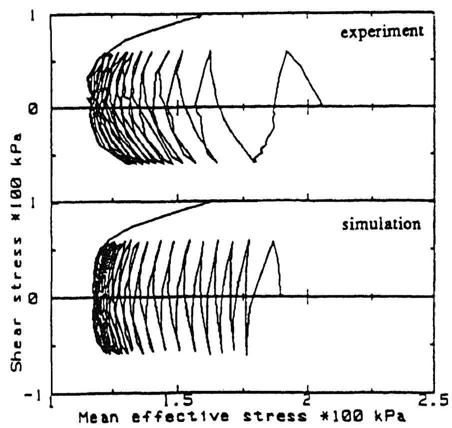

fig.6 Comparison between experiment and simulation cyclic loading between -τ_{max} and +τ_{max}

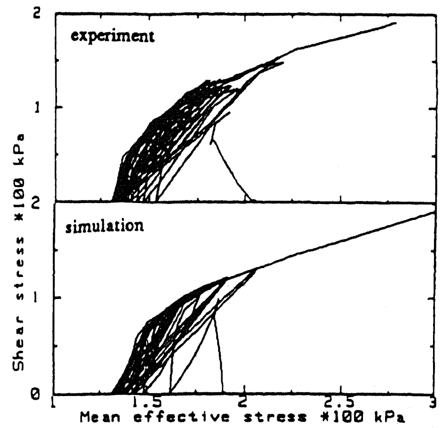

fig.7 Comparison between experiment and simulation, for 3 levels of compression cyclic loading

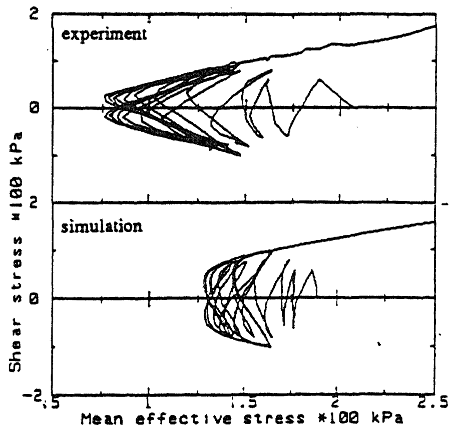

fig.8 Comparison between experiment and simulation for 3 levels of cyclic loading (between $-\tau_{max\ i}$ and $+\tau_{max\ i}$)

Different cyclic amplitudes are considered. Between 10 and 35 cycles are presented. We observe an increase of the pore pressure but, the liquefaction of the sand is not possible because a "limit" surface is reached for a non null mean effective stress.

For the different tests, the simulation reproduces correctly the shape of the experimental curve. Even quantitatively the two curves are close. The ability of the law to model complex phenomenon has to be underlined.

4 CONCLUSION

The non viscous part of the incremental rheological law of the "interpolation" type, for which no elastic domain is postulated, is presented. The interest of the developed law is that the whole stress path history is taken into account by the definition of three functions f, g, h. These functions replace the traditional elastic properties, yield surface(s) and plastic potential surface(s) introduced in the classical elastoplastic theory.

The law is quite "adaptable" because, with the change of some constants in the functions f, g, h, it allows to describe the behavior of other geomaterials. In function of the desired "sophistication" the number of constants may decrease.

The hollow cylinder apparatus developed for sand in our laboratory is described. This apparatus is able to apply stress paths with rotation of principal axes and allow:

- to study specifically stress paths with rotation of principal axes,
- to reproduce complex solicitations, close to the one observed in situ.

At least, the comparisons between numerical simulations with the law and experimental results show a good correlation for the different proposed stress paths. Complex phenomenon such as anisotropy and cyclic effects are described for stress paths with and without rotation of principal axes.

ACKNOWLEDGMENTS

This work has been sponsored by the CEC under contract n° CT 91-0046 and by the French Gréco Géomatériaux.

REFERENCES

Cazacliu G. B. 1991. Calibration du modèle incrémental de l'ENTPE sur sable. DEA ENTPE-INSA-ECL-UL

Chambon R. 1981. Contribution à la modélisation non linéaire des sols, Thèse de D.E., I.M. Grenoble

Darve F. 1978. Une formulation incrémentale des lois rhéologiques. Application aux sols, Thèse de D.E., Institut de Mécanique de Grenoble.

Di Benedetto H. 1981. Etude du comportement cyclique des sables en cinématique rotationnelle, Thèse de D.I. ENTPE-USMG.

Di Benedetto H. 1987. Modélisation du comportement des géomatériaux : application aux enrobés bitumineux et aux bitumes, Thèse de D.E. ENTP-USTMG-INPG.

Di Benedetto H. & Hameury O. 1991. Constitutive law for granular skeleton materials: description of the anisotropic and viscous effect, Comp. Meth. and Ad. in Geomec., ed. Booker & Carter, Balkema, 599-604

Doanh T., Di Benedetto H., Golcheh Y.& Kharchafi M. 1987. Non linear incremental constitutive equation: Application to sands. Constitutive Equations for Granular Non-Cohesive Soils, ed. Saada, Cleveland, Balkema, pp. 255-274.

Enrigen C. 1975. Continuum physics, Academic Press, New York, vol. 2, p. 615.

Ferry J.D. 1980. Viscoelastic properties of polymers, John Wiley and Sons.

Goldsheider M. 1982. Int. Workshop Cons. Behavior of Soils, Grenoble.

Hameury O., Di Benedetto H., Doanh T. & Ounaies W. 1991. Cycles non drainés de torsion: résultats expérimentaux et modélisation, Gréco Géomatériaux, Ed Reynouard JM., INSA Lyon

Kharchafi M. 1987. Contribution à l'étude du comportement des matériaux granulaires sous sollicitations rotationnelles, Thèse de Doctorat, ENTPE/ECP.

Kharchafi M. 1988. On effects of sample height in hollow cylinder tests. Constitutive Equations for Granular Non-Cohesive Soils, ed. Saada, Cleveland, Balkema, pp. 41-46.

Lanier J. 1988, 89 & 90. Gréco Géomatériaux, Ed Darve F., I.M. Grenoble, pp. 160-172 & 240-246.

Lanier J., Di Prisco C. & Nova R. 1991. Etude expérimentale et analyse théorique de l'anisotropie induite du sable d'Hostun, Revue Française de Géotechnique 57, pp. 59-74.

Royis P. 1986. Formulation mathématique de lois de comportement modélisation numérique de problèmes aux limites en mécanique des solides déformables , Thèse de D. I., INPG-ENTPE.